Journal of Biomedical Optics

BiomedicalOptics.SPIEDigitalLibrary.org

Hyperspectral near-infrared spectroscopy assessment of the brain during hypoperfusion

Thu Nga Nguyen
Wen Wu
Ermias Woldermichael
Vladislav Toronov
Steve Lin

SPIE.

Thu Nga Nguyen, Wen Wu, Ermias Woldermichael, Vladislav Toronov, Steve Lin, "Hyperspectral near-infrared spectroscopy assessment of the brain during hypoperfusion," *J. Biomed. Opt.* **24**(3), 035007 (2019), doi: 10.1117/1.JBO.24.3.035007.

Hyperspectral near-infrared spectroscopy assessment of the brain during hypoperfusion

Thu Nga Nguyen,[a,*] Wen Wu,[b,c] Ermias Woldermichael,[a] Vladislav Toronov,[a,d] and Steve Lin[b,c,d]
[a]Ryerson University, Faculty of Science, Department of Physics, Toronto, Ontario, Canada
[b]St. Michael's Hospital, Li Ka Shing Knowledge Institute, Toronto, Ontario, Canada
[c]University of Toronto, Department of Medicine, Toronto, Ontario, Canada
[d]Institute for Biomedical Engineering, Science and Technology, Toronto, Ontario, Canada

Abstract. Two-thirds of out-of-hospital cardiac arrest patients, who survive to hospital admission, die in the hospital from neurological injuries related to cerebral hypoperfusion. Therefore, noninvasive real-time monitoring of the cerebral oxygen metabolism in cardiac arrest patients is extremely important. Hyperspectral near-infrared spectroscopy (hNIRS) is a noninvasive technique that measures concentrations of the key chromophores in the brain, such as oxygenated hemoglobin, deoxygenated hemoglobin, and cytochrome C oxidase (CCO), an intracellular marker of oxygen consumption. We tested hNIRS on 10 patients undergoing transcatheter aortic valve insertion, where rapid ventricular pacing (RVP) is required to temporarily induce sudden hypotension and hypoperfusion that mimic cardiac arrest. Using multidistance hNIRS, we found that tissue oxygen saturation changes in the cerebral tissue were lower than those in the scalp during RVP. CCO redox changes were detected in cerebral tissue but not in the scalp during RVP. We have demonstrated that hNIRS is feasible and can detect sudden changes in cerebral oxygenation and metabolism in patients during profound hypotension. [DOI: 10.1117/1.JBO.24.3.035007]

Keywords: near-infrared spectroscopy; cardiac arrest; cytochrome c oxidase; cerebral oxygen saturation; transcatheter aortic valve insertion.

Paper 180525RR received Sep. 4, 2018; accepted for publication Jan. 23, 2019; published online Mar. 15, 2019.

1 Introduction

Out-of-hospital cardiac arrest occurs in over 350,000 people in North America and has a low survival rate of <10%.[1,2] Approximately two-thirds of out-of-hospital cardiac arrest patients who are resuscitated subsequently die in hospital due to neurological injuries, which are a result of prolonged hypoperfusion and ischemia.[3,4] There is a need to monitor cerebral perfusion and oxygenation. The American Heart Association has acknowledged that brain injury after cardiac arrest should be a critical focus in clinical research.[5] Cerebral monitoring is essential to provide optimal care to decrease ischemic brain injury after cardiac arrest.

There is currently no standard in measuring cerebral perfusion and oxygenation during cardiac arrest resuscitation. Near-infrared spectroscopy (NIRS) has recently been evaluated as a monitoring tool to measure cerebral oxygenation during and after cardiac arrest resuscitation.[6] NIRS is based on the measurement of the intensity of near-infrared light in the range of 700 to 1100 nm that passes through the skin, skull, scalp, and brain, which depends on the absorption and scattering coefficients of each tissue. The major chromophores absorbing near-infrared light are oxygenated hemoglobin (HbO_2), deoxygenated hemoglobin (Hb), fat, water, and cytochrome c oxidase (CCO).[7,8] The measurement of HbO_2 and Hb has been widely used to determine tissue oxygen saturation in the brain (tSO_2); however, CCO has been challenging to detect.[8] CCO plays a key role in the mitochondrial oxygen metabolism. While the total tissue concentration of CCO does not rapidly change over time, the changes in the difference between the concentrations of the oxidized and reduced forms of CCO (redox) can be measured based on the property that oxidized and reduced forms of CCO have different shapes of their absorption spectra.[8] The main challenge in measuring cerebral CCO redox changes (Δ[CCO]) is that CCO concentration is significantly lower compared to hemoglobin.[9] Commercially available NIRS devices use a few isolated wavelengths of near-infrared light [multispectral near-infrared spectroscopy (mNIRS)] instead of the full light spectrum, which may not be quantitatively accurate to measuring hemoglobin and CCO changes compared to using the whole broadband spectrum [hyperspectral near-infrared spectroscopy (hNIRS)].[9–13]

We have previously shown that changes in Δ[CCO] occurred during functional activations and when oxygen delivery was compromised.[12,14–18] hNIRS studies on humans have established evidence that Δ[CCO] has clinical relevance representing the metabolic state of brain cells and a measure of changes in cerebral oxygen delivery.[15,19–21] Using NIRS simultaneously with transcranial Doppler ultrasonography, Tisdall et al.[20] found a linear relationship between Δ[CCO] and cerebral oxygen delivery during hypoxemia in healthy adult humans. Δ[CCO] has also been shown to increase compared to microdialysate lactate/pyruvate ratios, a marker of anaerobic metabolism.[21] Using respiratory challenges, Holper and Mann[22] showed that Δ[CCO] responded to hypocapnia and hypercapnia that were comparable to hemodynamic changes. Nosrati et al.[12] found that in a porcine model of cardiac arrest, cardiopulmonary resuscitation (CPR) resulted in a higher increase in Δ[CCO] than in cerebral tissue oxygen saturation (tSO_2). Furthermore, in small observational studies, patients who survived after cardiac arrest had significantly higher cerebral tSO_2 compared to those who died.[23–25]

*Address all correspondence to Thu Nga Nguyen, E-mail: nga.nguyen@ryerson.ca

The objective of this study was to examine the feasibility of using hNIRS to detect sudden changes in cerebral oxygenation and metabolism in patients undergoing transcatheter aortic valve insertion (TAVI).[26] During a TAVI procedure, rapid ventricular pacing (RVP) is used to decrease stroke volume during balloon valvuloplasty and valve implantation. RVP can be used to model cardiac arrest as it produces periods of low flow or no flow perfusion states. hNIRS represents a technology that can help measure cerebral hemoglobin content and metabolism in the cardiac arrest patients and to determine the real-time cerebral response to CPR.

2 Materials and Methods

2.1 *Transcatheter Aortic Valve Insertion Patients and Procedure*

The study was approved by the St. Michael's Research Ethics Board (REB #14-397) and by the Ryerson University Research Ethics Board (REB #2016-177).

Ten patients consented to NIRS monitoring prior to their TAVI procedures. There were five male and five female patients with an average age of 82.6 years (range 74 to 87 years). NIRS monitoring was blinded to the treating physicians and did not alter treatment in any way. The TAVI procedure was performed by trained cardiothoracic surgeons in patients who were under general anesthesia. Clinical management was at the discretion of the anesthesiologist and cardiac surgery team.

Blood pressure and blood flow were significantly decreased during transient RVP via a temporary pacing wire to minimize left ventricular ejection and cardiac motion. RVP was induced in patients for ~10 to 30 s each time to help stabilize the valvuloplasty balloon during inflation and valve placement. When the anesthesiologist called out and initiated RVP, a research team member simultaneously marked the RVP on both the mNIRS and hNIRS devices.

2.2 *Near-Infrared Spectroscopy Setup*

Both hNIRS custom sensors (noninvasive stick pads) and mNIRS (Equanox 7600, Nonin, *Michigan*) were placed on each patient's forehead for the entire TAVI procedure. The hNIRS sensor was placed over the left forehead and the mNIRS sensor was applied onto the right forehead. A band was applied across the forehead to ensure contact of both sensors. The Equanox 7600 utilizes four wavelengths (730, 760, 810, and 880 nm) with four channels and uses calculations based on the Beer–Lambert law to determine tissue oxygen saturation (tSO_2).[27] The sensor has four mNIRS channels: two at 2 cm and two at 4 cm source–detector separations to exclude the influence of the skull and scalp on the measurement of the cerebral tSO_2.[27]

The hNIRS experimental setup of the TAVI procedure is shown in Fig. 1. The spectra were collected at the sampling rate of 2 Hz by two fiber optic spectrometers: QE 65000 and USB 4000 (Ocean Optics, Dunedin, Florida) at 3 and 1 cm, respectively, to separate the extracerebral and cerebral measurements. Both of these spectrometers had their range from 650 to 1100 nm. QE65000 had a high signal-to-noise ratio (1000:1 single acquisition) sufficient to measure light at 3-cm distance from the source. Two custom-made 2-m-long optical fiber bundles (each made of seven 0.5 NA, 400 μm core $\varnothing$ multimode polymer-clad fibers with broad UV/VIS/NIR spectral range of 400 to 2200 nm Thorlabs, New Jersey) connected spectrometers with the patient's head. The two other optical fiber bundles were used to connect the probe with a halogen lamp light source (Fiber-Lite Dc 950H Fiber Optic Illuminator, Dolan-Jenner, Massachusetts). The Spectra Suite (Ocean Optics, Florida) software was used to collect the broadband continuous-wave hNIRS data from both spectrometers with dark-signal correction.

2.3 *Hyperspectral Near-Infrared Spectroscopy Data Processing and Analysis*

hNIRS measures the absolute concentrations of tissue hemoglobin [HbO_2] and [Hb], and changes Δ[CCO]. hNIRS data acquired at 1- and 3-cm channels represented the extracerebral layer (scalp + skull) and a combined extracerebral and cerebral tissue volume, respectively. The data processing algorithm of hNIRS in our study was based on the analytical solution to the diffusion equation and implemented in MATLAB (MathWorks, Massachusetts, version R2016b).[12–13] The baseline concentrations of HbO_2, Hb, and water were determined using nonlinear least-square fitting[10] of the optical absorbance modeled as a function of the optical absorption coefficient $\mu_a(\lambda)$

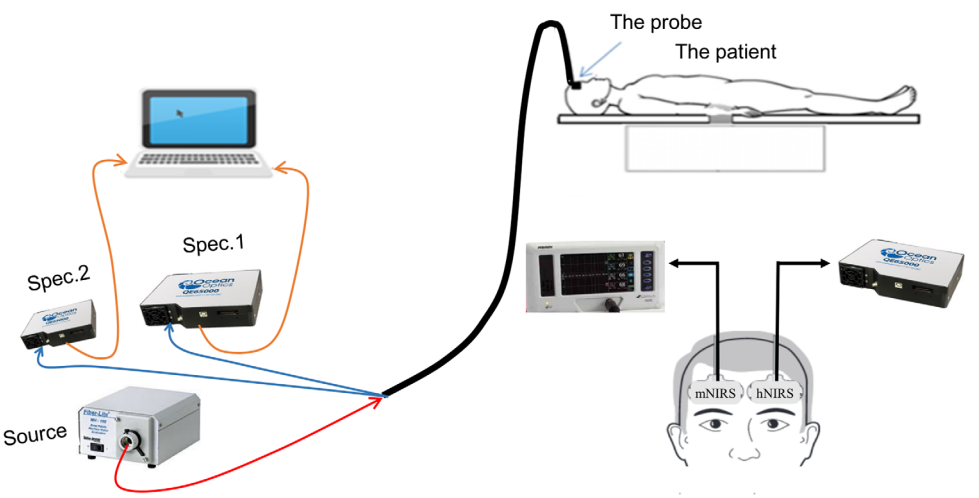

Fig. 1 TAVI experimental setup.

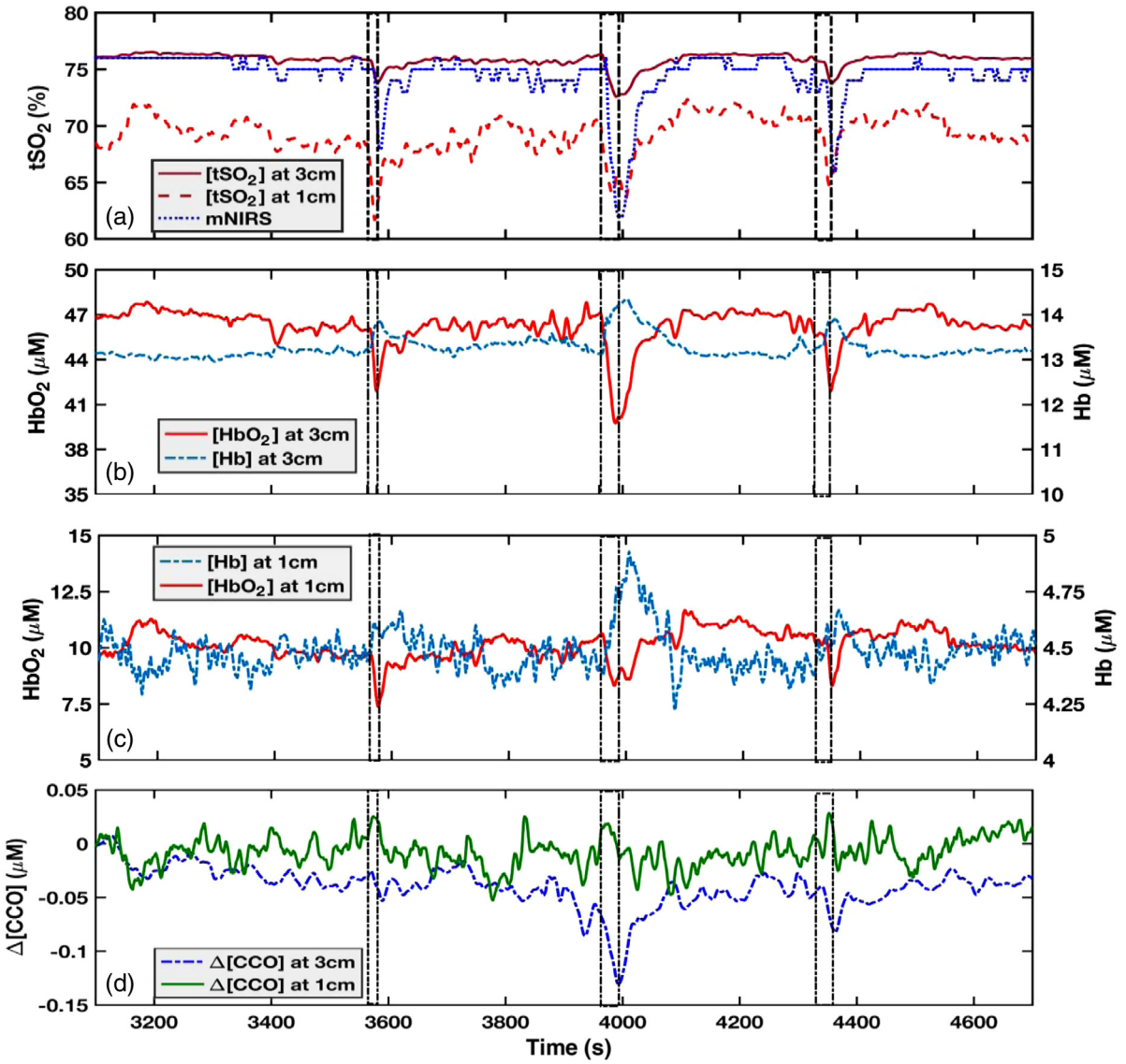

Fig. 2 Example of the time course of the changes during a TAVI procedure (patient 10) for: (a) [tSO_2] for hNIRS at the 1- and 3-cm channels and mNIRS device, (b) [HbO_2] and [Hb] changes at the 1-cm channel, (c) at 3-cm channel, and (d) Δ[CCO] at the 1- and 3-cm channels. Dashed lines indicate RVP episodes.

$$\mu_a(\lambda) = [\mathrm{Hb}]\varepsilon(\lambda)_{\mathrm{Hb}} + [\mathrm{HbO_2}]\varepsilon(\lambda)_{\mathrm{HbO_2}} + [\mathrm{H_2O}]\varepsilon(\lambda)_{\mathrm{H_2O}}, \tag{1}$$

and the reduced scattering coefficient $\mu_s'(\lambda)$ in the spectral band of 650 to 1000 nm. The reduced scattering coefficients (μ_s') were assumed to be independent of chromophore concentrations and were calculated for each wavelength (λ) using the power law, as described by Yeganeh et al.[10] Temporal changes in the hemoglobin concentrations HbO_2, Hb, and CCO redox were resolved using the time-spectral domain-independent component analysis for the signal denoising[28] and a multistep data-fitting algorithm[12,15] based on the analytical solution to the diffusion equation by relating changes in HbO_2, Hb, and CCO to the changes in the optical absorbance as

$$\Delta\mu_a(\lambda) = \Delta[\mathrm{Hb}]\varepsilon(\lambda)_{\mathrm{Hb}} + \Delta[\mathrm{HbO_2}]\varepsilon(\lambda)_{\mathrm{HbO_2}} + \Delta[\mathrm{CCO}]\varepsilon(\lambda)_{\mathrm{cco}}, \tag{2}$$

where $\varepsilon(\lambda)_x$ were the spectra of the extinction coefficients of HbO_2, Hb, and CCO redox.[29,30] The data fitting was performed is two steps. First, $\Delta[HbO_2]$ and Δ[Hb] were calculated assuming $\Delta[\mathrm{CCO}] = 0$ and second, Δ[CCO] was calculated and retained only if the addition of Δ[CCO] resulted in the improvement of the fit quality. Additional details on recovering the absolute values and changes of chromophore concentrations from the hNIRS data have been previously described.[10,12,15]

The cerebral tissue saturation of oxygen was calculated as the fraction of HbO_2 relative to the total hemoglobin in the blood:

$$\mathrm{tSO_2} = \frac{[\mathrm{HbO_2}]}{[\mathrm{HbO_2}] + [\mathrm{Hb}]}(\%). \tag{3}$$

The analysis of TAVI data using our homogenous model for the source–detector distances at 1 and 3 cm, respectively, was performed using MATLAB. All data were smoothed using the 0.5-Hz cutoff low-pass filter. Since tSO_2 showed prominent dips in the end of the RVP periods Fig. 2(a), we used the time of the

lowest tSO_2 value as a central timestamp for the calculation of the signal change during RVPs. To calculate changes in NIRS parameters produced by RVPs, we averaged their values X at five time points around the time of the lowest tSO_2 value during RVP and subtracted the average baseline values Y during 1 min prior to RVP. To assess the statistical significance of changes, we performed the left-tailed two-sample t-tests using the MATLAB function $[h, p] = ttest2(X, Y, \text{'Tail'}, \text{'left'})$, where h was the test outcome and p was the p-value.

3 Results

Changes in $[HbO_2]$, [Hb], tSO_2, and Δ[CCO] measured at 1 cm and 3 cm by hNIRS were typical for all patients. We show these changes in one sample TAVI patient (Fig. 2). $[HbO_2]$, tSO_2, and Δ[CCO] showed rapid decrease while [Hb] showed an increase during three RVP episodes, which lasted for 20, 28, and 24 s, respectively. The longest (second) RVP caused significantly larger responses in all parameters compared to the first and third RVP.

Both $[HbO_2]$ and [Hb] measured by the 1-cm channel were lower compared to the 3-cm channel [Figs. 2(b) and 2(c)].

Table 1 The hNIRS and mNIRS measured cerebral hemodynamics and metabolism for the 1- and 3-cm channels during RVP.

	CCO response in 3 cm channel (hNIRS)		ΔtSO_2 (%)		
Patient no.	CCO response detected	Δ[CCO] (μM)	mNIRS	3-cm hNIRS	1-cm hNIRS
1	Y($p < 0.001$)	−0.07	−13	−1.4	−4.3
2	Y($p = 0.02$)	−0.04	−9	−2.1	−10
3	Y($p < 0.001$)	−0.21	−13	−3.4	−16
	Y($p = 0.02$)	−0.08	−5	−1.3	−5.0
4	N($p = 0.3$)	0.01	−5	−2.4	−10
5	N($p = 0.4$)	−0.01	−9	−2.8	−5.2
6	Y($p = 0.01$)	−0.14	−10	−5.2	−9.7
	Y($p < 0.001$)	−0.49	−13	−6.0	−12
7	N($p = 0.12$)	−0.07	−10	−4.0	−4.6
	Y($p = 0.01$)	−0.14	−9	−2.7	−4.1
8	N($p = 0.07$)	−0.06	−10	−1.9	−3.1
	Y($p = 0.006$)	−0.10	−18	−3.7	−4.5
9	N($p = 0.4$)	−0.01	−13	−2.5	−5.7
	Y($p = 0.001$)	−0.09	−11	−2.6	−6.0
10	N($p = 0.6$)	0.00	−7	−2.1	−6.5
	Y($p = 0.001$)	−0.06	−13	−3.6	−6.0
	Y(0.02)	−0.04	−9	−2.7	−5.5
Average		-0.10 ± 0.07	-10 ± 3	-3.0 ± 0.3	-7.0 ± 0.8

The average changes during RVP in $[HbO_2]$ and [Hb] were $\sim 5.2 \pm 1.97$ μM and 0.92 ± 0.26 μM, respectively, at the 3-cm channel and 2.3 ± 2.3 μM and 0.28 ± 0.33 μM, respectively, at the 1-cm channel. Δ[CCO] decreased significantly at the 3-cm channel during the second and third RVPs, whereas Δ[CCO] at the 1-cm channel did not show significant changes during RVP ($p > 0.1$) [Fig. 2(d)].

Baseline values of tSO_2 measured by hNIRS at 1- and 3-cm channels and by mNIRS channels were between 70% and 76%. The time course of all three tSO_2 measurements showed similar trends during and after RVPs with significant decrease at the end of each RVP ($p < 0.01$). The magnitude of tSO_2 changes during RVPs measured by the mNIRS, and 1-cm hNIRS channels were similar and higher than at the 3-cm hNIRS channel. On average, tSO_2 at 1-cm channel decreased by $6.95\% \pm 0.79\%$, compared to $2.96\% \pm 0.30\%$ at 3-cm channel.

The measurements of tSO_2 and Δ[CCO] during RVPs for all 10 TAVI patients are summarized in Table 1. Δ[CCO] measured by the 3-cm hNIRS channel showed significant drops (0.1 ± 0.07 μM on average, $p < 0.05$) during 12 RVP episodes in 8 patients, whereas Δ[CCO] measured by the 1-cm channel was never significant ($p > 0.05$). The correlation coefficients between Δ[CCO] and ΔtSO_2 are shown in Table 2. The highest correlation 0.7 ± 0.2 was between Δ[CCO] and ΔtSO_2 measured by hNIRS at 3 cm.

4 Discussion

We measured cerebral oxygen saturation and metabolism using hNIRS in TAVI patients during transient periods of RVP, which can be used to model the low flow or no flow states of cardiac arrest. Overall, we observed significant changes in $[HbO_2]$, [Hb], and tSO_2 during RVP, which were consistent with previously published studies.[26,31–33] Δ[CCO] decreased during RVP, which may represent changes in the intracellular oxygen consumption by cerebral cells.[8,17–18,31]

The 1-cm channel reflected the changes in the noncerebral tissue, such as scalp and skull, and the 3-cm channel measured both the noncerebral tissue and the cerebral cortex. Interestingly, tSO_2 decreased during RVPs but not Δ[CCO] at the 1-cm channel. This may have been due to the brain being more sensitive to profound hypotension, even during short intervals of RVP, compared to the scalp. The metabolic rate is also higher in the brain compared to skin and muscle,[32] which may help to explain these results. Decreases in brain Δ[CCO] may occur only after longer periods of hypotension if RVPs lasted longer in our TAVI patients. Alternatively, since the oxygen metabolic rate is higher in the brain[20,33,34] and hemodynamic noise at small separations was higher than at larger separations,[35] our hNIRS monitor may not have detected these small changes at the 1-cm distance.

In two patients, Δ[CCO] changes were not measured in both the 1- and 3-cm detector distances. This may have been due to smaller changes in Δ[CCO] that were not detected by our sensors compared to other patients in this study. Alternatively, as the brain atrophies with increased age, there is a need to increase detector separation (>3 cm) in order to penetrate brain parenchyma.[36,37] Okada and Delpy[38] suggested that the increased cerebrospinal fluid could substantially affect the penetration of near-infrared light into the brain. Furthermore, the average differential path-length factor also increases with age due to the higher scattering in extracerebral tissue.[39]

We found that ΔtSO_2 measured by hNIRS at 3 cm ($\sim 2.96\%$) was lower than at 1 cm ($\sim 6.95\%$) despite the reverse in HbO_2.

Table 2 The correlation coefficients between values from Table 1.

	Δ[CCO] 3-cm hNIRS	Δ[tSO_2] 3-cm hNIRS	Δ[tSO_2] mNIRS	Δ[tSO_2] 1-cm hNIRS
Δ[CCO] 3-cm hNIRS	1	0.7 ± 0.2	0.4 ± 0.3	0.5 ± 0.3
Δ[tSO_2] 3-cm hNIRS	0.7 ± 0.2	1	0.4 ± 0.3	0.4 ± 0.3
Δ[tSO_2] mNIRS	0.4 ± 0.3	0.4 ± 0.3	1	0.4 ± 0.5
Δ[tSO_2] 1-cm hNIRS	0.5 ± 0.3	0.4 ± 0.3	0.4 ± 0.5	1

This may have been due to the differences in the proportion of vasculature (with higher [HbO2] and [Hb]) in the scalp and skull compared to the brain. This heterogeneity could limit the quantitative accuracy of cerebral tSO_2 changes by hNIRS. The cerebral tSO_2 as measured by mNIRS monitor may in fact be more reliable due to the calibration of Equanox 7600 for the influence of the skull and scalp.[27]

Our results agree with previous NIRS studies comparing magnetic resonance imaging,[40] time-resolved spectroscopy measurement, and Monte Carlo simulations.[16] These studies found that hemodynamic changes correlated with the cerebral hemoglobin signal in the extracerebral tissues. Monte Carlo simulations[16] showed that the largest amount of detected photons propagating into the adult brain was from a 3-cm source–detector separation. However, Δ[CCO] was less prone to extracerebral contamination and more specific to mitochondrial concentration.[33] Our results also agree with Kolyva et al.[17] who found that Δ[CCO] increased with longer source–detector distances in four different experimental settings: hypoxia, hyperoxia, hypocapnia, and hypercapnia.

This study had several limitations. The biological and optical properties and the thickness of the noncerebral tissue likely varied between patients, which was not determined in this study. Although this was beyond the scope of this study, we plan to apply a two-layer model to our data measured at 1- and 3-cm separations to improve the accuracy of measuring [HbO2], [Hb], tSO_2, and Δ[CCO].[11] The application of a two-layer model may better evaluate the differences in the brain compared to the scalp and skull. Moreover, future studies will be performed to determine the optimal distances between optodes to accurately measure [HbO2], [Hb], tSO_2, and Δ[CCO] in the brain.

5 Conclusion

We have shown that hNIRS is sensitive to sudden changes in tSO_2, [HbO_2], [Hb], and Δ[CCO] during profound hypoperfusion in TAVI patients. The changes in CCO redox measured by hNIRS were more specific marker of cerebral status than tSO_2.

Disclosures

The authors have no relevant financial interests in this article and no potential conflicts of interest to disclose.

Acknowledgments

We gratefully acknowledge the physicians and patients from St. Michael's Hospital for their support in this study. This study was supported by the Heart and Stroke Foundation of Canada Emerging Research Leaders Initiative grant and the St. Michael's Foundation Translational Innovation Fund. S.L. is a network investigator of the Cardiac Arrhythmia Network of Canada (CANet) and was supported by a Heart and Stroke Foundation of Canada Ontario Clinician-Scientist award.

References

1. G. Nichol, E. Thomas, and C. W. Callaway, "Regional variation in out-of-hospital cardiac arrest incidence and outcome," *JAMA* **300**(12), 1423–1431 (2008).
2. B. McNally et al., "Out-of-hospital cardiac arrest surveillance—Cardiac Arrest Registry to Enhance Survival (CARES), United States, October 1, 2005–December 31, 2010," *MMWR Surveill. Summ.* **60**(8), 1–19 (2011).
3. R. Neumar et al., "Post-cardiac arrest syndrome: epidemiology, pathophysiology, treatment, and prognostication. A consensus statement from the International Liaison Committee on Resuscitation (American Heart Association, Australian and New Zealand Council on Resuscitation, European Resuscitation Council, Heart and Stroke Foundation of Canada, InterAmerican Heart Foundation, Resuscitation Council of Asia, and the Resuscitation Council of Southern Africa); the American Heart Association Emergency Cardiovascular Care Committee; the Council on Cardiovascular Surgery and Anesthesia; the Council on Cardiopulmonary, Perioperative, and Critical Care; the Council on Clinical Cardiology; and the Stroke Council," *Circulation* **118**(23), 2452–2483 (2008).
4. S. Laver et al., "Mode of death after admission to an intensive care unit following cardiac arrest," *Intensive Care Med.* **30**(11), 2126–2128 (2004).
5. G. Frohlich et al., "Out-of-hospital cardiac arrest—optimal management," *Curr. Cardiol. Rev.* **9**(4), 316–324 (2014).
6. A. Cournoyer et al., "Near-infrared spectroscopy monitoring during cardiac arrest: a systematic review and meta-analysis," *Acad. Emerg. Med.* **23**(8), 851–862 (2016).
7. F. Jobsis, "Noninvasive, infrared monitoring of cerebral and myocardial oxygen sufficiency and circulatory parameters," *Science* **198**(4323), 1264–1267 (1977).
8. G. Bale, C. Elwell, and I. Tachtsidis, "From Jöbsis to the present day: a review of clinical near-infrared spectroscopy measurements of cerebral cytochrome-c-oxidase," *J. Biomed. Opt.* **21**(9), 091307 (2016).
9. R. Thiele et al., "Broadband near-infrared spectroscopy can detect cyanide-induced cytochrome aa_3 inhibition in rats: a proof of concept study," *Can. J. Anesth.* **64**(4), 376–384 (2017).
10. H. Yeganeh et al., "Broadband continuous-wave technique to measure baseline values and changes in the tissue chromophore concentrations," *Biomed. Opt. Express* **3**(11), 2761–2770 (2012).
11. O. Pucci, V. Toronov, and K. St. Lawrence, "Measurement of the optical properties of a two-layer model of the human head using broadband near-infrared spectroscopy," *Appl. Opt.* **49**(32), 6324–6332 (2010).
12. R. Nosrati et al., "Cerebral hemodynamics and metabolism during cardiac arrest and cardiopulmonary resuscitation using hyperspectral near infrared spectroscopy," *Circ. J.* **81**(6), 879–887 (2017).
13. R. Nosrati et al., "Simultaneous measurement of cerebral and muscle tissue parameters during cardiac arrest and cardiopulmonary resuscitation," *Proc. SPIE* **9305**, 93051G (2015).
14. C. E. Cooper et al., "Use of mitochondrial inhibitors to demonstrate that cytochrome oxidase near-infrared spectroscopy can measure mitochondrial

dysfunction noninvasively in the brain," *J. Cereb. Blood Flow Metab.* **19**(1), 27–38 (1999).
15. R. Nosrati et al., "Event-related changes of the prefrontal cortex oxygen delivery and metabolism during driving measured by hyperspectral fNIRS," *Biomed. Opt. Express* **7**(4), 1323–1335 (2016).
16. Y. Hoshi et al., "Reevaluation of near-infrared light propagation in the adult human head: implications for functional near-infrared spectroscopy," *J. Biomed. Opt.* **10**(6), 064032 (2005).
17. C. Kolyva et al., "Cytochrome c oxidase response to changes in cerebral oxygen delivery in the adult brain shows higher brain-specificity than haemoglobin," *NeuroImage*. **85**(1), 234–244 (2014).
18. T. Sanderson et al., "Inhibitory modulation of cytochrome c oxidase activity with specific near-infrared light wavelengths attenuates brain ischemia/reperfusion injury," *Sci. Rep.* **8**(1), 3481 (2018).
19. A. Bakker et al., "Near-infrared spectroscopy," in *Applied Aspects of Ultrasonography in Humans*, P. Ainslie, Ed., InTech (2012).
20. M. Tisdall et al., "Near-infrared spectroscopic quantification of changes in the concentration of oxidized cytochrome c oxidase in the healthy human brain during hypoxemia," *J. Biomed. Opt.* **12**(2), 024002 (2007).
21. M. Tisdall et al., "Increase in cerebral aerobic metabolism by normobaric hyperoxia after traumatic brain injury," *J. Neurosurg.* **109**(3), 424–432 (2008).
22. L. Holper and J. Mann, "Test-retest reliability of brain mitochondrial cytochrome-c-oxidase assessed by functional near-infrared spectroscopy," *J. Biomed. Opt.* **23**(05), 056006 (2018).
23. F. Nomura et al., "Cerebral oxygenation measured by near infrared spectroscopy during cardiopulmonary bypass and deep hypothermic circulatory arrest in piglets," *Pediatr. Res.* **40**(6), 790–796 (1996).
24. J. C. Schewe et al., "Monitoring of cerebral oxygen saturation during resuscitation in out-of-hospital cardiac arrest: a feasibility study in a physician staffed emergency medical system," *Scand. J. Trauma Resusc. Emerg. Med.* **22**(15), 58 (2014).
25. A. Frisch et al., "Potential utility of near-infrared spectroscopy in out-of-hospital cardiac arrest: an illustrative case series," *Prehospital Emerg. Care* **16**(1), 564–570 (2012).
26. A. Miceli et al., "Minimally invasive aortic valve replacement with a sutureless valve through a right anterior mini-thoracotomy versus transcatheter aortic valve implantation in high-risk patients," *Eur. J. Cardio-Thoracic Surg.* **49**(3), 960–965 (2016).
27. D. MacLeod et al., "Development and validation of a cerebral oximeter capable of absolute accuracy," *J. Cardiothorac. Vasc. Anesth.* **26**(6), 1007–1014 (2012).
28. I. Schelkanova and V. Toronov, "Independent component analysis of broadband near-infrared spectroscopy data acquired on adult human head," *Biomed. Opt. Express* **3**(1), 64–74 (2012).
29. S. Matcher et al., "Performance comparison of several published tissue near-infrared spectroscopy algorithms," *Anal. Biochem.* **227**(1), 54–68 (1995).
30. G. Liao and G. Palmer, "The reduced minus oxidized difference spectra of cytochromes a and a3," *Biochim. Biophys. Acta* **1274**(3), 109–111 (1996).
31. M. Ferrari and V. Quaresima, "A brief review on the history of human functional near-infrared spectroscopy (fNIRS) development and fields of application," *NeuroImage* **63**(2), 921–935 (2012).
32. Z. Wang et al., "Specific metabolic rates of major organs and tissues across adulthood: evaluation by mechanistic model of resting energy expenditure," *Am. J. Clin. Nutr.* **92**(6), 1369–1377 (2010).
33. Y. Kakihana et al., "Brain oxymetry in the operating room: current status and future directions with particular regard to cytochrome oxidase," *J. Biomed. Opt.* **13**(3), 033001 (2008).
34. M. Smith and C. Elwell, "Near-infrared spectroscopy: shedding light on the injured brain," *Anesth. Analg.* **108**(4), 1055–1057 (2009).
35. T. Germon et al., "Extracerebral absorption of near infrared light influences the detection of increased cerebral oxygenation monitored by near infrared spectroscopy," *J. Neurol. Neurosurg. Psychiatry* **58**(4), 477–479 (1995).
36. D. L. Greenberg, D. L. Fetzer, and M. E. Payne, "Aging, gender, and the elderly adult brain: an examination of analytical strategies," *Neurobiol. Aging* **29**(2), 290–302 (2008).
37. S. M. Resnick et al., "Longitudinal magnetic resonance imaging studies of older adults: a shrinking brain," *J. Neurosci.* **23**(1), 3295–3301 (2003).
38. E. Okada and D. Delpy, "Near-infrared light propagation in an adult head model. II. Effect of superficial tissue thickness on the sensitivity of the near-infrared spectroscopy signal," *Appl. Opt.* **42**(16), 2915 (2003).
39. F. Scholkmann and M. Wolf, "General equation for the differential pathlength factor of the frontal human head depending on wavelength and age," *J. Biomed. Opt.* **18**(10), 105004 (2013).
40. A. Kleinschmidt et al., "Simultaneous recording of cerebral blood oxygenation changes during human brain activation by magnetic resonance imaging and near-infrared spectroscopy," *J. Cereb. Blood Flow Metab.* **16**(5), 817–826 (1996).

Thu Nga Nguyen received her MSc degree in biomedical physics from Ryerson University. She is a member of SPIE and has presented her research work at SPIE conferences.

Wen Wu is a fourth-year medical student from the University of Toronto. He previously graduated from the University of Ottawa with a bachelor's degree in biochemistry. He is currently interested in emergency medicine and resuscitation research.

Ermias Woldermichael holds his MSc degree in biomedical physics by Ryerson University, Toronto, Ontario. His focus is on the use of hyperspectral near-infrared spectroscopy to study functional brain activity and mild traumatic brain injury.

Vladislav Toronov received PhD in physics from Saratov State University, Russia. He was a research scientist in biomedical physics at the University of Illinois at Urbana-Champaign. Currently, he is associate professor of physics, Ryerson University, Toronto, Canada, member of the Institute for Biomedical Engineering, Science and Technology (iBEST) of Ryerson University and St. Michael's Hospital. Research interests include brain imaging and optical spectroscopy and imaging of tissue.

Steve Lin is an emergency physician, trauma team leader, and scientist in the Li Ka Shing Knowledge Institute of St. Michael's Hospital. He is an assistant professor and clinician-scientist in the Division of Emergency Medicine, Department of Medicine at the University of Toronto. He is establishing a research program of translational science to optimize resuscitation during cardiac arrest or life-threatening injuries and to develop drug therapies and devices for goal-directed therapy in resuscitation.